

# EVOLUTION OF DISK ACCRETION

NURIA CALVET\* and LEE HARTMANN  
*Harvard-Smithsonian Center for Astrophysics*

and

STEPHEN E. STROM  
*Five College Astronomy Department, University of Massachusetts\*\**

We review the present knowledge of disk accretion in young low mass stars, and in particular, the mass accretion rate  $\dot{M}$  and its evolution with time. The methods used to obtain mass accretion rates from ultraviolet excesses and emission lines are described, and the current best estimates of  $\dot{M}$  for Classical T Tauri stars and for objects still surrounded by infalling envelopes are given. We argue that the low mass accretion rates of the latter objects require episodes of high mass accretion rate to build the bulk of the star. Similarity solutions for viscous disk evolution suggest that the inner disk mass accretion rates can be self-consistently understood in terms of the disk mass and size if the viscosity parameter  $\alpha \sim 10^{-2}$ . Close companion stars may accelerate the disk accretion process, resulting in accretion onto the central star in  $\leq 1\text{Myr}$ ; this may help explain the number of very young stars which are not currently surrounded by accretion disks (the weak emission T Tauri stars).

## I. INTRODUCTION

The initial angular momenta of star-forming molecular cloud cores must be responsible for the ultimate production of binary (and multiple) stellar systems and circumstellar disks. Unless the protostellar cloud core is very slowly rotating, much or most of the stellar mass is likely to land initially on a disk, and must subsequently be accreted from the disk onto the protostellar core. In the early phases of this accretion, the circumstellar disks may be relatively massive in comparison with the central protostar, and so gravitational instabilities may be important in angular momentum transport and consequent disk evolution. At later phases, disk evolution is likely to be driven by viscous processes, perhaps limited by condensation of bodies. Stellar magnetic fields may ultimately halt the accretion of material onto the central

---

\* Also Centro de Investigaciones de Astronomía

\*\* Now at National Optical Astronomy Observatories

star. There are substantial uncertainties in our theoretical understanding of these processes, and we must rely on observations for guidance.

In this chapter we review the present knowledge of the disk accretion process around low mass stars, in particular the rate at which mass is transferred onto the star,  $\dot{M}$ , and its evolution with time. Knowledge of  $\dot{M}$  will help put lower limits on the disk mass at a given age, independent of uncertainties in dust opacities. It puts constraints on disk physics, and in particular on temperatures and surface densities at a given age, and thus on conditions which obtain during the time when solid bodies agglomerate. We begin with a description of the different methods of determining disk accretion rates and the values of  $\dot{M}$  obtained applying these methods to stars in different groups and environments. We then discuss the implications of the observational results for disk accretion physics and evolution, and in particular investigate whether the data are consistent with simple models of viscous disk evolution.

## II. DETERMINATION OF $\dot{M}$

### A. Infrared excesses

When the infrared excess emission in Classical T Tauri stars (hereafter CTTS) was recognized as emission from dust at low temperatures distributed in a circumstellar disk, it was thought that the excess energy would be a direct measurement of the accretion luminosity ( $L_{acc} = G\dot{M}M_*/R_*$ , where  $M_*$  and  $R_*$  are the stellar mass and radius). However, it soon became apparent that their spectral energy distributions (SEDs) did not follow the law  $\lambda F_\lambda \propto \lambda^{-4/3}$  expected for standard accretion disks, but were much flatter (Rydgren and Zak 1987; Kenyon and Hartmann 1987). It has now been realized that the major agent heating the disks of many CTTS is irradiation by the central star (Adams and Shu 1986; Kenyon and Hartmann 1987; Calvet et al. 1991, 1992; Chiang and Goldreich 1997; D'Alessio et al. 1998). The optically-thick disks of CTTS are probably “flared”, i.e., have “photospheres” that curve away from the disk midplane; this makes them more efficient in absorbing light from the central star; this extra heating helps to increase the disk scale height and thus increases the flaring. Self-consistent calculations (in various approximations) indicate that the flaring is especially important at large radii (Kenyon and Hartmann 1987; Chiang and Goldreich 1997; D'Alessio et al. 1998). This makes it extremely difficult, if not impossible, to say anything about accretion energy release, and thus accretion rates, in outer disk emission.

For many CTTS it is very difficult to extract quantitative estimates of mass accretion rates even from emission from the inner, flat parts of the disk. The basic reason is that the accretion luminosities of many

CTTS are smaller than the luminosity the optically-thick inner disk produces as a result of absorbing light from the central star.

The effective temperature  $T$  of the disk is determined by internal viscous dissipation and external irradiation by the central star; at a given annulus,

$$T^4(r) \sim T_v^4 + T_i^4, \quad (1)$$

where  $T_v = [(3GM_*\dot{M}/8\pi\sigma r^3)f]^{1/4}$  is the effective temperature that would result from accretion without irradiation, with  $f = 1 - \sqrt{(R_*/r)}$ , and  $T_i^4 = (2/3\pi)T_*^4(R_*/r)^3$  is the effective temperature for the case of only irradiation (the flat disk approximation). In these expressions, we assume that the mass accretion rate through the inner disk is constant and equal to the rate at which mass is transferred onto the star. The mass accretion rate at which  $T_i \sim T_v$  is

$$\dot{M}_c \sim 2 \times 10^{-8} M_\odot \text{yr}^{-1} (T_*/4000\text{K})^4 (R_*/2R_\odot)^3 (M_*/0.5M_\odot)^{-1},$$

calculated for typical Taurus CTTS parameters (K7-M0, age  $\sim 1$  Myr) and  $r \sim 3R_*$ . Since the median value of  $\dot{M}$  in CTTS is  $\sim 10^{-8} M_\odot \text{yr}^{-1}$  (see below), this implies that irradiation dominates the inner disk heating for a large number of the stars and determines the amount of flux excess. Only for objects with significantly high  $\dot{M}$  will the (near-infrared) disk emission depend upon the mass accretion rate.

Other considerations affect a disk's near-infrared emission. It was originally thought that CTTS disks extended all the way into the star, and disk material joined the star through a "hot boundary layer", where half of the accretion energy was dissipated, while the other half was emitted in the disk (cf. Bertout 1989). It has now become apparent that for typical values of the stellar magnetic field ( $< 1$  kG, Basri et al. 1992) and of the mass accretion rate, the inner disk of CTTS can be disrupted by the magnetic field (Königl 1991; Najita et al., this volume); material falls onto the star along the magnetic field lines, forming a magnetosphere, and merges with the star through an accretion shock at the stellar surface. In support of this model, fluxes and line profiles of the broad (permitted) emission lines in CTTS are well explained by the magnetospheric flow (Calvet and Hartmann 1992; Hartmann et al. 1994; Edwards et al. 1994; Muzerolle et al. 1998a,b,c; Najita et al., this volume), while the ultraviolet and optical excess fluxes are well accounted for by the accretion shock emission (Calvet and Gullbring 1998).

For truncation radii  $R_i \sim 3 - 5 R_*$ , the maximum temperature in a disk with typical parameters will be  $\sim 1200 - 850\text{K}$ , so that disk emission drops sharply below  $\sim 2 - 3.5\mu\text{m}$ . The calculation of the disk luminosity from the observed excess also depends upon the cosine of the inclination angle, which is generally unknown. As an illustration of

these points, Meyer et al. (1997) have shown that the so-called “CTTS locus” in JHK and HKL diagrams, i.e., the region populated by CTTS outside that corresponding to reddened main sequence stars (Meyer et al., this volume) could be explained in terms of emission by irradiated accretion disks with inner holes of different sizes (but inside co-rotation radii), and a random distribution of inclinations. However, no one-to-one correlation could be found between the excess and  $\dot{M}$ . In a sample of stars in Taurus with known reddening and  $\dot{M}$ , the largest excesses in the locus were produced by stars with the highest  $\dot{M}$ , but the converse was not true, due to the effects of holes and inclination.

Finally, in objects surrounded by infalling dusty envelopes, emission from the dust destruction radius, which peaks at  $\sim 2\mu\text{m}$ , may contribute significantly to the K band and longward (Calvet et al. 1997), hiding the intrinsic disk emission.

The difficulty of deriving reliable measures of  $\dot{M}$  from excess infrared emission requires using alternative methods of estimating  $\dot{M}$ 's. We will consider such methods in the next two sections.

## B. Veiling luminosities

The best evidence for CTTS disk accretion generally comes from the interpretation of the ultraviolet and optical spectra. The photospheric absorption lines are “veiled”, that is, they are less deep than standard stars of the same spectral type. This veiling is produced by (mostly) continuum emission from a region hotter than the stellar photosphere. The luminosity of the veiling or excess continuum in CTTS is typically  $\sim 10\%$  of the total stellar luminosity. It is difficult to account for this extra energy with a stellar origin, and impossible in the case of most extreme CTTS, where the excess continuum luminosity is several times the stellar luminosity. This conclusion is reinforced by the existence of the weak-emission T Tauri stars or WTTS. The WTTS have similar masses and ages as the CTTS in many regions, but do not exhibit the UV-optical veiling continuum of CTTS, showing that the excess emission is not an intrinsic property of young stars. The veiling emission is observed only when there is excess near-infrared emission (Hartigan et al. 1995; Najita et al., this volume), strongly supporting the idea that accretion from a disk is occurring, producing both the infrared excess as well as the hot continuum, as originally envisaged by Lynden-Bell and Pringle (1974).

In the magnetospheric model, the disk is truncated in the inner regions, which is precisely where an accretion disk would emit most of its energy. The total disk accretion luminosity is expected to be about

$$L_{acc}(disk) \sim GM_*\dot{M}/(2R_i) + L_{diss}$$

where  $L_{diss}$  is any energy that might be dissipated in the disk by the stellar magnetic field lines (Kenyon et al. 1996). If we assume that the

effect of the stellar magnetic field is to substantially reduce the angular momentum of the disk material, so that it starts out nearly at rest at  $R_i$  before falling onto the star along the magnetic field lines, then the infalling material should dissipate its energy at the stellar surface at a rate  $\sim (GM_*\dot{M}/R_*)(1 - R_*/R_i)$ . For disk truncation radii  $\sim 3 - 5R_*$ , most of the accretion energy is released at the stellar surface in the hot accretion shock whose radiation is observed as the veiling continuum (Königl 1991; Calvet and Gullbring 1998).

Accretion luminosities can be obtained from measurements of the veiling of the absorption lines by the following procedure in which excess and intrinsic photospheric emission components are separated. The observed fluxes are fitted by the scaled, dereddened fluxes of a standard star, assumed to be of the same spectral type as the object star, plus a continuum flux, which produces the observed veiling at each absorption line wavelength. This fit yields the spectrum of the excess continuum and the reddening towards the star. The total excess luminosity is calculated from the measured luminosity using a model to extrapolate the emission to unobserved wavelengths. Finally, the mass accretion rate can be calculated from stellar mass and radius estimated from the location of the star in the HR diagram and comparison with evolutionary tracks.

Accretion luminosities for CTTS in Taurus have been determined from veiling measurements by a number of authors, including Hartigan et al. (1991), Valenti et al. (1993), and Hartigan et al. (1995). The mass accretion rates derived from these studies range from  $\sim 10^{-7}M_\odot yr^{-1}$  for Hartigan et al., to  $\sim 10^{-8}M_\odot yr^{-1}$  for Valenti et al. More recently, Gullbring et al. (1998, GHBC), re-measured accretion rates for a sample of Taurus CTTS using spectrophotometry covering the blue and Balmer jump region of the spectrum down to the atmospheric cutoff, and found their results to agree with the previous lower estimates. In a sample of 17 CTTS in Taurus, GHBC found a median value of  $\dot{M} \sim 10^{-8}M_\odot yr^{-1}$ , with a factor of  $\sim 3$  in estimated error.

These differences reflect the cumulative effects of a number of differences in working assumptions rather than a fundamental difference in approach. Among them we can list the following: (1) Adopted evolutionary tracks; (2) Adopted model of accretion. The magnetosphere model predicts more luminosity per mass accretion rate than the old boundary layer model; (3) Adopted physics. Some treatments assumed that a substantial fraction of the emitted accretion energy was absorbed by the star, which seems unlikely (Hartmann et al. 1997); (4) Differing methods used to determine extinction corrections. The photospheres of T Tauri stars show color anomalies relative to standards, which render the determination of reddening uncertain. In particular, GHBC found large color anomalies in some non-accreting WTTS often used as templates; this would cause the extinction to be overestimated in

all objects. These anomalies are probably due to spots on the stellar surface and/or unresolved, cooler companion stars.

To provide a powerful tool to determine mass accretion rates for large samples of stars for which short wavelength spectrophotometry is difficult to obtain, GHBC determined the relationship between the accretion luminosity and the excess luminosity in the U photometric band,  $L_U$ , for the stars in their sample. Figure 1a shows the excellent relationship between  $\log L_{acc}$  and  $\log L_U$ . A least-squares fit to the line yields:

$$\log(L_{acc}/L_{\odot}) = 1.04_{-0.18}^{+0.04} \log(L_U/L_{\odot}) + 0.98_{-0.07}^{+0.02} \quad (2)$$

The spectrophotometric sample from which equation (2) was derived is formed by stars in the K5-M2 range, with most of the stars being K7-M0. The application of this calibration to a wider spectral type/mass range remains to be confirmed, but theoretical models of accretion shock emission from stars of differing mass and radii indicate that for the characteristic energy fluxes found in the accretion columns of CTTS, the spectrum of the excess emission does not depend on the underlying star, and the proportion of the total excess luminosity in the U band ( $\sim 10\%$ ) displayed by equation (2) holds (Calvet and Gullbring 1998).

Mass accretion rates have been determined for a larger sample of TTS in Taurus using equation (2) by Hartmann et al. (1998, HCGD). The median mass accretion rate is  $\sim 10^{-8} M_{\odot} yr^{-1}$ , similar to that of the spectrophotometric sample, but the errors are larger, given the lack of simultaneity in the photometric measurements and the high degree of variability of CTTS. HCGD also used spectral types and photometry from the compilation of Gauvin and Strom (1992) to estimate mass accretion rates for K5-M3 stars in the Chamaeleon I association. The median mass accretion rate in Chamaeleon I is  $\sim 4 \times 10^{-9} M_{\odot} yr^{-1}$ . A histogram of the mass accretion rate for TTS in Taurus and Chamaeleon I determined from the ultraviolet excess is presented in Fig. 2a.

### C. Magnetospheric emission lines

The measurement of mass accretion rates from the optical and ultraviolet excess fluxes, either spectrophotometrically or from broad-band photometry, is sensitive to reddening corrections. In heavily-extincted stars, the UV fluxes are either very uncertain or unobservable; thus, in early stage of evolution such as the infall/protostellar phase, or in very young, dense regions of star formation, such methods cannot be used. For these objects, it is necessary to devise methods to measure  $\dot{M}$  in spectral regions that are less affected by intervening dust.

Most emission lines present in the spectra of young objects are thought to be produced in the magnetospheric flow (Najita et al., this

volume). Since the material flows through the magnetosphere with a rate similar to  $\dot{M}$  in the inner disk, the emission fluxes of the lines formed in this flow are expected to depend upon the mass accretion rate. Theoretical models show this to be the case, but other parameters, such as the unknown temperature structure and the characteristic size play a role too, as well as the optical depth of the line (Muzerolle et al. 1998a). For these reasons, empirical correlations between line luminosities and accretion luminosities have been investigated, leaving the interpretation to future theoretical work.

Muzerolle et al. (1998b,c, MHCb,c) have undertaken spectroscopic studies in the red and infrared of the sample of stars with accretion rates determined from spectrophotometric measurements, and have found remarkably good correlations between the luminosity of the Ca II triplet 8542, Pa $\beta$ , and Br $\gamma$  lines with accretion luminosities. Figure 1b show the correlation between  $L_{acc}$  and the luminosity in Br $\gamma$ , as an example. Least-squares fits to the data give:

$$\log(L_{acc}/L_{\odot}) = (0.85 \pm 0.12) \log(L_{CaII8542}/L_{\odot}) + (2.46 \pm 0.46), \quad (3)$$

$$\log(L_{acc}/L_{\odot}) = (1.03 \pm 0.16) \log(L_{Pa\beta}/L_{\odot}) + (2.80 \pm 0.58), \quad (4)$$

and

$$\log(L_{acc}/L_{\odot}) = (1.20 \pm 0.21) \log(L_{Br\gamma}/L_{\odot}) + (4.16 \pm 0.86). \quad (5)$$

These subsidiary calibrators of the accretion rate provide the means to determine accretion rates in heavily extincted objects for the first time.

MHCc used luminosities of the Br $\gamma$  line for extincted Class II sources in  $\rho$  Oph from Greene and Lada (1996) to make the first determination of accretion luminosities for these sources. They find that the distribution of accretion luminosities is similar to that in Taurus. Using approximate spectral types from Greene and Meyer (1995), the estimated median mass accretion rate is  $\sim 1.5 \times 10^{-8} M_{\odot} yr^{-1}$ , although the span of spectral types covered is wider than in the Taurus sample.

Even more far reaching, MHCc determined accretion luminosities for the deeply embedded Class I objects (sources still surrounded by infalling envelopes) for the first time, using Br $\gamma$  luminosities. Since typically  $A_V \sim 20 - 30$  for Class I objects, significant extinction is expected at Br $\gamma$  ( $A_K \sim 2 - 3$ ), which introduces large uncertainties in the determination of the line luminosities. The light from the central star+disk and from the envelope itself is absorbed *and* scattered by the infalling envelope, in proportions that depend on uncertain parameters such as the geometry of the inner envelope (Calvet et al. 1997). Following Kenyon et al. (1993b), MHCc calculate a correction factor K-K0, by assuming that the central object has J-K colors similar to

CTTS, and estimating the intrinsic J magnitude from the bolometric luminosity.

Figure 3 shows accretion luminosities estimated by MHCc for a small number of Class I sources in Taurus and in  $\rho$  Oph which have data on Br $\gamma$  (Greene and Lada 1996) plotted against the total luminosities. The accretion luminosities of Class I sources are significantly lower than the system bolometric luminosity; in fact, the mean accretion luminosity is  $\sim 10 - 20\%$  of the mean bolometric luminosity of the sample. This fact implies that the luminosity of Class I is dominated by the stellar component, and gives a natural explanation to the similarity of the distributions of luminosities of Class I and optically visible T Tauri stars in Taurus (Kenyon et al. 1990).

Determining the mass accretion rate from  $L_{acc}$  requires knowledge of  $M_*/R_*$ . We can obtain this ratio assuming that the stars are still on the birthline (Stahler 1988), which seems justified since they are still accumulating mass from the envelope/disk. We used the observed bolometric luminosity to locate the object along the birthline (calculated for an infall rate of  $2 \times 10^{-6} M_\odot yr^{-1}$ ). Figure 2b shows the distribution of  $\dot{M}$  thus obtained for Class I sources in Taurus and  $\rho$  Oph.

The mean mass infall rate in the envelope,  $\dot{M}_i$ , has been estimated in Taurus from fitting the spectral energy distributions and scattered light images of Class I sources to be  $\sim 4 \times 10^{-6} M_\odot yr^{-1}$  (Kenyon et al. 1993a), a value which is consistent with theoretical expectations (Shu et al. 1987). The present determination of disk accretion rate shown in Fig. 2b indicates that many Class I objects are slowly accreting from their disks, despite the fact that mass is being deposited in the outer disk at a higher rate. This discrepancy was first recognized by Kenyon et al. (1990), as the so-called luminosity problem of Class I sources. If infall were spherical, the luminosity of the system would be given by an accretion luminosity  $\sim GM_*\dot{M}_i/R_*$ . But in this case, the predicted accretion luminosity should be of order  $10L_\odot$ , while the mean luminosity of Taurus Class I sources is  $\sim 1 - 2L_\odot$  (Kenyon et al. 1990, 1994). Kenyon et al. (1990) pointed out that the mass accretion rate in the disk onto the star does not necessarily equal the mass infall rate from the envelope onto the disk, since they are regulated by different physical processes. The imbalance between the infall and accretion rates in this picture leads to an accumulation of mass in the disk. These disks could eventually become gravitationally unstable (Larson 1984), with consequent rapid accretion until sufficient mass has been emptied out of the disk. Kenyon et al. (1990) suggested that these episodes could be related to the FU Orionis outbursts.

#### D. The FU Ori disks

The FU Orionis outbursts are now recognized as a transient phase of high mass accretion in the disk around a forming low mass star



(see review by Hartmann and Kenyon 1996 and references therein). Although so far FU Ori objects have been mostly studied as isolated phenomena, it is becoming increasingly clear that episodes of high mass accretion rate may be a crucial, if not dominant, process in the formation of stars. We briefly review here the determination of  $\dot{M}$  for these objects.

The canonical FU Ori objects were discovered from their increase in brightness by several magnitudes over time scales of months to years (Herbig 1977), during which the luminosity increased from values typical to CTTS to a few hundred  $L_{\odot}$ . Since the emission is dominated by the accretion disk in FU Ori objects, the accretion luminosity can be readily determined from the observed SED. Additional information is required to independently obtain  $M_*/R_*$  and  $\dot{M}$ , which can be estimated from the surface temperature in the inner disk ( $R \sim 2 - 3 R_*$ ),  $T_{max} \sim 7000K(L_{acc}/100L_{\odot})^{1/4}(R_*/2R_{\odot})^{1/2}$  (from  $T_v$  in equation [1]), and measurements of the rotational velocity. Using this method,  $\dot{M} \sim 10^{-4}M_{\odot}yr^{-1}$  has been inferred for the canonical objects for which outbursts have been observed, consistent with their high luminosities,  $> 100L_{\odot}$ .

A significant number of objects have been identified as FU Ori objects in recent years, mostly at IR wavelengths. Photometric variability indicative of outbursts has been detected in only a few objects; their classification as FU Ori systems has been based mostly on the presence of the near-infrared first overtone bands of CO in deep absorption, comparable to late type giants and supergiants and to the canonical FU Ori objects. Most of these objects are in very early stages of evolution, as is their prototype L1551 IRS 5, embedded in infalling envelopes and associated with Herbig-Haro objects, jets and/or molecular outflows (Elias 1978, Graham and Frogel 1985, Reipurth 1985; Staude and Neckel 1991; Kenyon et al. 1993; Hanson and Conti 1995; Hodapp et al. 1996; Reipurth and Aspin 1997; Sandell and Aspin 1998). The luminosities of the objects identified so far as members of the FU Ori class range from  $\sim 10L_{\odot}$  to  $800L_{\odot}$ . Since  $\dot{M} \sim 2 \times 10^{-6}M_{\odot}yr^{-1}(L_{acc}/10L_{\odot}) \times [(M_*/R_*)/0.18M_{\odot}/R_{\odot}]^{-1}$ , this range implies  $\dot{M} \geq \text{few} \times 10^{-6}M_{\odot}yr^{-1}$  (assuming they are on the birthline, with typical  $M_*/R_* \sim 0.18M_{\odot}/R_{\odot}$ ). This value is consistent with the presence of CO in absorption, since disk atmosphere calculations indicate that the temperature of the continuum forming region is higher than the surface temperature (neglecting any wind contribution) for  $\dot{M} > 10^{-6}M_{\odot}yr^{-1}$  (Calvet et al. 1992).

The nature of the low luminosity FU Ori objects and their relationship to the canonical objects remains to be elucidated. One possibility is that disks undergo instabilities driving outbursts of different magnitude. Alternatively, these objects could be in the phase of decay from a

canonical FU Ori outburst. An argument in favor of the second possibility comes from comparison of the mass loss rate required to drive the molecular outflow and the present mass accretion rate. For L1551 IRS5 and PP13S ( $L = 10L_{\odot}$  and  $30L_{\odot}$ , respectively), the momentum flux of the molecular flow is  $\sim \text{few} \times 10^{-4} M_{\odot} \text{yr}^{-1} \text{kms}^{-1}$ . (Moriarty-Schieven and Snell 1988; Sandell and Aspin 1997). For typical velocities of the jet of  $\text{few} \times 100 \text{kms}^{-1}$ , and assuming momentum conservation, the momentum flux implies mass loss rates of the same order to the inferred mass accretion rates, while both theoretically and observationally, the ratio between the mass loss rate and mass accretion rate is close to  $\sim 0.1$  (Calvet 1997). This discrepancy may imply that the mass accretion rate of the disk was much higher when the material giving rise to the molecular outflow was ejected.

### III. THE EVOLUTION OF ACCRETION

#### A. Observed $\dot{M}$ vs. age

Figure 4 shows mass accretion rate vs. age for CTTS in Taurus,  $\rho$  Oph, and Chamaeleon I, for which significant infall from an envelope has stopped. We also show the range of  $\dot{M}$  covered by Class I sources in Taurus, assuming a median age of 0.1 Myr (estimated from the ratio of the number of Class I sources to T Tauri stars in Taurus, and adopting a mean age of 1 Myr for the latter, Kenyon et al. 1990). The data indicates a clear trend of accretion decaying with time (HCGD; see also Hartigan et al. 1995), even in the relatively short age spread covered by the observations. There is also a very large spread in mass accretion rate at a given age, which makes it very difficult to quantify the rate of decay. HCGD shows that the slope of a least-squares-fit to the data is highly dependent on the errors of  $\dot{M}$  and age. If errors are assumed larger in  $\dot{M}$  than in age (the most likely situation, cf. HCGD), then the slope is  $\approx -1.5$  (with large uncertainty).

#### B. Disk Masses

We can use the observed mean decay of  $\dot{M}$  with time to obtain an estimate for the mass of the disk for comparison with masses estimated from dust emission. The amount of mass accreted by a CTTS from the present time to infinity constitutes a lower limit to the mass remaining in the disk. If  $\dot{M}(t) \sim \dot{M}(t_o)(t/t_o)^{-\eta}$ , then this limit to the disk mass is  $M_{acc} = \dot{M}(t_o)t_o/(\eta - 1) \sim 2\dot{M}(t_o)t_o$ , with  $\eta \sim 1.5$ . This gas mass can be compared to the disk mass estimated from dust emission in the submillimeter and millimeter range,  $M_{mm}$ , which is very dependent on the assumed opacities (Beckwith et al. 1990; Osterloh and Beckwith 1995, masses corrected by a factor of 2.5, HCGD). The comparison (for single stars) yields  $\log(2\dot{M} \times \text{age}/M_{mm}) = -0.07 \pm 0.21$ , indicating that masses inferred from the current mass accretion rates and age estimates,

which are probing the gas, are consistent with disk masses estimated independently from mm-wave dust opacities, which in turn suggests that the dust opacities used in the latter estimates are appropriate.

### C. Early stages

Figure 4 indicates that the mean mass accreted onto the star during the CTTS phase is  $\sim 10^{-2}M_{\odot}$ . This suggests that by the time stars reach the optically visible CCTS stage, the remaining disk mass is relatively low and little mass is added to the forming star. This picture implies that the bulk of stellar accretion must occur during the (highly-extincted) infall phase, when the disk is being continually replenished by the collapsing envelope. However, during the infall phase, our results suggest that disk accretion rates during quiescent phases are only slightly higher than those in the CTTS stage, precluding addition of more than  $\sim 0.01M_{\odot}$  during these phases. Significant additions to the mass of the growing protostar must therefore come via material accreted during transient episodes of high accretion.

André et al. (1993) suggest that the Class 0 objects are in the earliest phases of envelope collapse, when central accretion rates are expected to be the highest, and argue that the Class 0 sources are the true protostars. These very heavily extincted objects have somewhat higher luminosities than the mean Class I luminosity in Taurus, and so may have higher accretion rates onto the central star. However, Class 0 sources tend to be less frequent than Class I sources, especially in Taurus; thus, the lifetime of the Class 0 phase may be too short to account for most of the stellar accretion.

The high accretion rate episodes required to explain the accretion of the stellar mass can be attributed to instabilities in quiescent low  $\dot{M}$  disks, which result in outbursts and transient periods of high mass accretion rates. Several models have been presented to trigger those outbursts. The most accepted model is that of thermal instabilities in the inner disk (Lin and Papaloizou 1985; Clarke et al. 1990; Kawazoe and Mineshige 1993; Bell and Lin 1994; Bell et al. 1995). This model can naturally explain the occurrence of outbursts during the infall phase because it requires a high background mass accretion rate from the outer disk, of the order of a few  $\times 10^{-6}M_{\odot}yr^{-1}$ , to match the observations. Moreover, according to this model outbursts will be triggered in the disk as long as mass is deposited in the outer disk at this rate, ensuring that mass will be transferred from the initial cloud into the star.

The number of currently-known FU Ori objects is insufficient to explain the formation of typical stars mostly through outbursts (Hartmann and Kenyon 1996). However, the known sample of FU Ori disks is very incomplete, because the identifying characteristic of high mass accretion rate disks is the near-infrared bands of CO in absorption and

many objects may be too heavily extinguished to be detected at  $\sim 2.2\mu\text{m}$ . More and more sensitive observations of embedded objects in the near-infrared are necessary to test this hypothesis.

#### D. Viscous evolution in TTS disks

Once the main infall phase is over and the envelope is no longer feeding mass and angular momentum into the disk, we expect disk evolution to be driven mostly by viscous processes, namely, those in which the angular momentum transport is provided by a turbulent viscosity. In this and the next section, we attempt to interpret the observed properties of CTTS disks in terms of viscous evolution, with the aim of understanding the main physical processes at play and the role of initial and boundary conditions. Similarly, physical models for disk evolution help us relate properties and evolution of the inner disk, as measured by  $\dot{M}(t)$ , to those of the outer disk, such as radius and mass,  $R_d$  and  $M_d$ .

The disk angular momentum is

$$J_d = \int_0^{M_d} dM \Omega R^2 \propto M_d R_d^{1/2}. \quad (6)$$

where  $\Omega$  is the Keplerian angular velocity. If we neglect the (small amount) of angular momentum being added to the star, or the possible angular momentum loss to an inner disk wind (Shu et al. 1994; Shu et al., this volume), then the disk angular momentum is approximately constant. In turn, this requires  $R_d \propto M_d^{-2}$ , so angular momentum conservation implies that the disk expands as the mass of the disk is accreted to the star. Evolution occurs on the viscous time scale,  $t_{\text{visc}} \sim R^2/\nu$ , where  $\nu$  is the viscosity (Pringle 1981). If  $\nu \propto R^\gamma$ , then  $dR_d/dt \sim R_d/t_{\text{visc}} \propto R_d^{\gamma-1}$ , so  $R_d \propto t^{1/(2-\gamma)}$ ,  $M_d \propto t^{-1/2(2-\gamma)}$ , and  $\dot{M} \propto t^{-(5/2-\gamma)/(2-\gamma)}$ . Therefore and in principle, from the observed decay of  $\dot{M}$  with time,  $\dot{M}(t) \propto t^{-\eta}$ , we can obtain  $\gamma = (2\eta - 5/2)/(\eta - 1)$ , and the evolution of radius and mass of the disk can be predicted.

As Lynden-Bell and Pringle (1974) showed, analytic similarity solutions describing the evolution of disk properties exist for the case of power-law viscosity (see also Lin and Bodenheimer 1982). These analytical similarity solutions have been applied by HCGD as a first approximation to the evolution of T Tauri disks. (More complex models have been used by Stepinski (1998) to consider similar issues; whether the observational constraints justify approaches with more assumed parameters is not clear.) HCGD argue that the use of a power-law viscosity can be justified on approximate grounds. Using the  $\alpha$  prescription for the viscosity (Shakura and Sunyaev 1973),  $\nu = \alpha c_s H \propto c_s^2/\Omega(R) \propto T(R)R^{3/2}$ , where  $c_s$  is the sound speed and  $H$  the scale height. If  $T(R) \propto R^{-q}$ , then  $\nu \propto R^{3/2-q}$ . With  $q \sim 1/2$ , corresponding

to irradiated disks at large distances from the star (Kenyon and Hartmann 1987; D’Alessio et al. 1998), and also found by empirical fitting to apply to most disks in CTTS (Beckwith et al. 1990), then  $\gamma \sim 1$ , which is roughly consistent with the observed slope of the  $\dot{M}$  vs. age data,  $\eta \approx 1.5$  (section III.A).

HCGD calculated similarity solutions for viscous evolution for a range of initial conditions applicable to CCTS disks. Figures 5a and 5b show the evolution of mass accretion rate and disk mass for a subset of models in this study. Initial disk masses have been taken as  $M_d(0) = 0.1M_\odot$ , consistent with small disk masses remaining after disk-draining episodes of high  $\dot{M}$  (III.C). Values for other values of  $M_d(0)$  can be obtained by simple scaling. Model results are shown for three values of the initial radius, 1, 10, and 100 AU, which cover an order of magnitude in angular momentum, consistent with the spread of angular momentum between half of the binaries in the solar neighborhood (Duquennoy and Mayor 1991). The calculations assume a temperature of 10 K at 100 AU, as suggested by irradiated disk calculations (D’Alessio et al. 1998), and a central stellar mass of  $0.5M_\odot$ . The viscosity parameter  $\alpha$  has been taken as 0.01, except when stated otherwise. The observed values of disk masses and mass accretion rates, shown in Fig. 5a and 5b lie within the region bounded by the assumed range of initial conditions. Disks with larger initial radii take longer to start evolving, since the viscous time scale is  $t_{visc} \sim R^2/\nu \propto R$ .

The surface density of the similarity solutions behaves with radius as

$$\Sigma \propto \frac{e^{-(R/R_1)/(t/t_s)}}{(R/R_1)}, \quad (7)$$

where  $R_1$  and  $t_s$  are characteristic radius and time (see HCGD for details); it goes like  $\propto R^{-1}$  at small radii and falls sharply at large distances. This last property determines important differences in the disk “sizes” measured at different wavelengths, and naturally explains the observed disparity between the optical and mm sizes. Disk radii measured at millimeter wavelengths are of the order of a few hundred AU (Dutrey et al. 1996), while the radii of the disks seen in silhouettes in the Orion Nebula cluster at  $0.6 \mu\text{m}$  are much larger,  $\sim 500 - 1000$  AU (McCaughrean and O’Dell 1996).

Figure 6 shows the predicted radii of models in Fig. 5 at 2.7 mm and  $0.6\mu\text{m}$ , compared to the observations. Circles indicate the Dutrey et al. (1996) observations, while the error bar indicates the range of sizes of the Orion silhouettes. To calculate the millimeter sizes the two-dimensional brightness distribution of the disk model has been convolved with a Gaussian with the appropriate beam size. Radii at other wavelengths correspond to the radii where the optical depth is  $\sim 1$  at the given wavelength (HCGD). The theoretical predictions compare

well with the observations. Since dust opacity increases rapidly towards the optical, the outer tenuous regions of the disk can effectively absorb background light and produce a large apparent size. In contrast, in the millimeter range these outer cooler, low density regions contribute little to the surface brightness and the observed sizes are consequently smaller (HCGD). The larger millimeter size of the disk in the binary (open circle) may be indicative of a circumbinary disk, for which the present calculations do not apply.

Figure 6 shows the predicted size of one of the models at  $1.87\mu\text{m}$ . At an age of  $\sim 0.5\text{Myr}$ , typical of the Orion Nebula cluster, the infrared sizes are  $\sim 20\%$  smaller than the optical sizes, in good agreement with observations (McCaughrean et al. 1998). The sharp decline of surface density with radius predicted by viscously evolving models naturally explains the observed sizes, without the need for heavily truncated edges.

Figure 6 also shows with long dashes the predictions for the observed sizes in the millimeter range of a disk model with  $\alpha = 0.001$ . Since  $t_{\text{visc}} \sim R^2/\nu \propto 1/\alpha$ , disks with small  $\alpha$  take much longer to start evolving and growing, resulting in sizes much smaller than observed at the typical ages of the young population. Thus, measurements of disk sizes as a function of time will place important constraints on the characteristic value of  $\alpha$  in CTTS disks.

Disk evolution could be considerably different if angular momentum is lost from outer disk regions through a wind (e.g., Pudritz and Norman 1983, Königl 1989). We have argued elsewhere (Hartmann 1995) that this is not the case. Similarly, coagulation of disk material into bodies that sweep clear the gas will significantly modify this simple picture of disk evolution. Nevertheless, it is encouraging that the observations can be explained with a viscosity ( $\alpha \sim 10^{-2}$ ) comparable to that estimated in simulations of the Balbus-Hawley magnetorotational instability (Stone et al. 1996; Brandenburg et al. 1996).

## E. Effects of companion stars

There is a large spread in the mass accretion rates and disk masses as a function of age. Some of this range is probably due to uncertainties in age determinations, errors in accretion rates (for example, due to ignoring inclination effects), time-variability, and a range in initial conditions. However, the potential effects of companion stars cannot be ignored; since at least  $\sim 2/3$  of all systems are binaries (Duquennoy and Mayor 1991), it is important to consider the effects of a binary companion on the evolution of disk accretion when comparing with observations.

A companion star may prevent the formation of a disk in its immediate vicinity, and will try to open gaps on either side of its orbit (cf. Artymowicz and Lubow 1994, AL; Lubow and Artymowicz, this

volume). While the “initial” effects of a binary companion can strongly limit disk structure and accretion, it is important to realize that there may be secondary effects as well. Specifically, even with a relatively distant companion, the inner structure of a viscously-evolving disk will eventually be affected by the companion, even though the tidal forces are negligible in this region. The reason is that the isolated viscously-evolving disk can only accrete if its outer regions expand to take up the necessary angular momentum. In the similarity solution described above, the mass accretion rate decreases as a power-law in time, because as the disk empties out it also expands and thus has an increasingly long viscous time. In contrast, if a binary companion limits the expansion of the disk, once the disk reaches its maximum size, the viscous time remains constant, and so the (inner) regions empty out exponentially with time. (Note that these considerations are relevant only to circumstellar disks, not circumbinary disks, which can expand.)

Figures 5c and 5d show a very simple calculation of this type of effect, using the same power-law viscosity used in the standard model, but now not allowing the disk to expand beyond a certain outer radius, using the boundary conditions discussed by Pringle (1991). One observes that when the disk expands to the limiting radius, the accretion rate first increases slightly, and then drops precipitously as the disk empties out rapidly.

The significance of this estimate can be seen by noting that the median binary separation is roughly 30 AU (Duquennoy and Mayor 1991). With the reference disk model used, and estimating a truncation radius  $\sim 1/3$  of the binary separation ( $AL$ ), this would mean that even if all binaries originally had circumstellar disks, half of those binaries would have their disks empty out by an age of 1 Myr. These estimates are roughly consistent with the percentage of  $\sim 1$  Myr WTTS in Taurus,  $\sim 45\%$  (Kenyon and Hartmann 1995); the predicted fraction of WTTS could be even higher if indeed the fraction of binaries in Taurus is higher than in the solar neighborhood (Simon et al. 1995).

These estimates of binary effects on disk evolution are rough, and the model ignores the effects of the (significant) eccentricities of binary orbits ( $AL$ ), but they serve to illustrate the importance of identifying stellar companions to understand disk evolution in individual systems. Figures 5c and d do not show a very strong correlation of mass accretion rates with binarity, though there is a significant effect on disk masses (cf. Jensen et al. 1994; Mathieu et al. 1995; Osterloh and Beckwith 1995). In any case, many of the systems shown have not been studied carefully for potential companions, and in general much work remains to be done in this area.

#### IV. SUMMARY AND IMPLICATIONS

Figure 7 summarizes the ideas presented so far in a sketch of disk evolution with time for a single star. After maybe a short initial period of high mass accretion rate, the disk remains most of the time in a quiescent state. Episodes of high mass accretion rate are triggered mostly during the phase where the disk is still immersed in the infalling envelope, in which we expect most of the star to be built. After the infall ceases and the star emerges as a T Tauri star, the disk evolves viscously,  $\dot{M}$  slowly decreases with time, at the same time that the disk expands and its mass decreases.

There are several implications of these results for star and planet formation. First, disk accretion during the protostar phase appears to be highly variable. This may call into question theories of the birth-line, or the initial position of stars in the HR diagram (Stahler 1988; Hartmann et al. 1997), which assume steady accretion at the rates of infall of the protostellar envelope. It is conceivable that planetesimals or other bodies form in the disk during this phase but are swept into the star as the disk accretes, perhaps partly accounting for some of the accretion variability - our observations really only probe energy release in the inner disk, near the star. Second, there appears to be a wide variety of disk masses and accretion rates (say, a range of an order of magnitude) during the T Tauri phase, produced in part by differences in initial angular momenta. This may mean that any consequent planetary systems which form could have quite different properties. Third, the ability of viscous accretion disk models to explain the observations so far suggests that substantial migration of material occurs during the T Tauri phase; this migration as disks actively accrete may be important in explaining some of the extrasolar planets which lie close to their star. Fourth, the presence of binary companions obviously does not always prevent disk formation, but they may accelerate (circumstellar) disk accretion. Improved mm and submm interferometry, as well as infrared speckle searches for companion stars and improved radial velocity studies to search for close, low-mass stellar companions, will lead to a greatly improved understanding of disk evolution.

#### Acknowledgements

We thank a number of people for useful discussions and valuable insight, including James Muzerolle, Erik Gullbring, Paola D'Alessio, Cesar Briceño, Ray Jayawardhana, Suzan Edwards, Lynne Hillenbrand, Michael Meyer, Bo Reipurth, and David Wilner. This work was supported in part by NASA grant NAG5-4282.



## REFERENCES

- Adams, F. C. and Shu, F. H. 1986. Infrared Spectra of Rotating Protostars. *Astrophys. J.* 308:836-853.
- André, P., Ward-Thompson, D., and Barsony, M. 1993. Submillimeter continuum observations of Rho Ophiuchi A - The candidate protostar VLA 1623 and prestellar clumps. *Astrophys. J.* 406:122-141.
- Artymowicz, P. and Lubow, S. H. 1994, Dynamics of binary-disk interaction. 1: Resonances and disk gap size. *Astrophys. J.* 421:651-667.
- Basri, G., Marcy, G.W. and Valenti, J. A. 1992. Limits on the magnetic flux of pre-main sequence stars. *Astrophys. J.* 390:622-633
- Beckwith, S. V. W., Sargent, A. I., Chini, R. S. and Guesten, R. 1990. A survey for circumstellar disks around young stellar objects. *Astron. J.* 99:924-945.
- Bell, K. R. and Lin, D. N. C. 1994. Using FU Orionis outbursts to constrain self-regulated protostellar disk models. *Astrophys. J.* 427:987-1004.
- Bell, K. R., Lin, D. N. C, Hartmann, L. and Kenyon, S. J. 1995. The FU Orionis outburst as a thermal accretion event: Observational constraints for protostellar disk models. *Astrophys. J.* 444:376-395.
- Bertout, C. 1989. T Tauri stars - Wild as dust. *Ann. Rev. Astron. Astrophys.* 27:351-395.
- Bonnell, I. and Bastien, P. 1992, A binary origin for FU Orionis stars. *Astrophys. J.* 401:L31-L34.
- Brandenburg, A., Nordlund, A., Stein, R.F., and Torkelsson, U. 1996. *Astrophys. J.* 458:L45.
- Calvet, N., Patiño, A., Magris C., G. and D'Alessio, P. 1991. Irradiation of accretion disks around young objects. I - Near-infrared CO bands. *Astrophys. J.* 380:617-630.
- Calvet, Magris C., G., Patiño, A. and D'Alessio, P. 1992. Irradiation of Accretion Disks Around Young Objects. II. Continuum Energy Distribution. *Rev. Mex. Astron. Astrofis.* 24:27-42.
- Calvet, N. and Hartmann, L. 1992. Balmer line profiles for infalling T Tauri envelopes. *Astrophys. J.* 386:239-247.
- Calvet, N., Hartmann, L. and Strom, S. E. 1997. Near-Infrared Emission of Protostars. *Astrophys. J. Lett.* 481:912-917.
- Calvet, N. 1995 Properties of the Winds of T Tauri Stars. In *Herbig-Haro Flows and the Birth of Stars; IAU Symposium No. 182*, eds. B. Reipurth and C. Bertout. (Dordrecht: Kluwer Academic Publishers), p. 417-432.
- Calvet, N. and Gullbring, E. 1998, *Astrophys. J.* (in press)
- Chiang, E. I. and Goldreich, P. 1997. Spectral Energy Distributions of T Tauri Stars with Passive Circumstellar Disks *Astrophys. J.* 490:368-376.

- Clarke, C.J., Lin, C D.N.C. and Pringle, J. E. 1990. Pre-conditions for disc-generated FU Orionis outbursts. *Mon. Not. Roy. Astron. Soc.* 242:439-446.
- D'Alessio, P., Cantó, J., Calvet, N. and Lizano, S. 1998. Accretion Disks around Young Objects. I. The Detailed Vertical Structure. *Astrophys. J.* 500:411-427.
- D'Antona, F. and Mazitelli, I. 1994. New pre-main-sequence tracks for M less than or equal to 2.5 solar mass as tests of opacities and convection model. *Astrophys. J. Suppl.* 90:467-500.
- Duquennoy, A. and Mayor, M. 1991. Multiplicity among solar-type stars in the solar neighbourhood. II - Distribution of the orbital elements in an unbiased sample. *Astron. Astrophys.* 248:485-524.
- Dutrey, A., Guilloteau, S., Duver, G., Prato, L., Simon, M., Schuster, K. and Menard, F. 1996. Dust and gas distribution around T Tauri stars in Taurus-Auriga. I. Interferometric 2.7mm continuum and  $CO_{13}$  J=1-0 observations. *Astron. Astrophys.* 309:493-504.
- Edwards, S., Hartigan, P., Ghandour, L. and Andrulis, C. Spectroscopic evidence for magnetospheric accretion in classical T Tauri stars. *Astron. J.* 108:1056-1070.
- Elias, J. H. 1978. A study of the IC 5146 dark cloud complex. *Astrophys. J.* 223:859-875.
- Gauvin, L. S. and Strom, K. M. 1992. A study of the stellar population in the Chamaeleon dark clouds. *Astrophys. J.* 385:217-231.
- Graham, J.A. and Frogel, J. A. 1985. An FU Orionis star associated with Herbig-Haro object 57. *Astrophys. J.* 289:331-341.
- Greene, T. P. and Lada, C. J. 1996. Near-Infrared Spectra and the Evolutionary Status of Young Stellar Objects: Results of a 1.1-2.4 micron Survey. *Astron. J.* 112:2184-2221.
- Greene, T. P. and Meyer, M. R. 1995. An Infrared Spectroscopic Survey of the rho Ophiuchi Young Stellar Cluster: Masses and Ages from the H-R Diagram. *Astrophys. J.* 450:233-244.
- Gullbring, E., Hartmann, L., Briceño, C. and Calvet, N. 1998 Disk Accretion Rates for T Tauri Stars. *Astrophys. J.* 492:323-341.
- Hanson, M. M. and Conti, P. S. 1995. Identification of Ionizing Sources and Young Stellar Objects in M17. *Astrophys. J. Lett.* 448:L45-L48.
- Hartigan, P., Strom, S. E., Edwards, S., Kenyon, S. J., Hartmann, L., Stauffer, J. and Welty, A. D. 1991. Optical excess emission in T Tauri stars. *Astrophys. J.* 382:617-635.
- Hartigan, P., Edwards, S. and Ghandour, L. 1995. Disk Accretion and Mass Loss from Young Stars. *Astrophys. J.* 452:736-768.
- Hartmann, L., Hewett, R. and Calvet, N. 1994. Magnetospheric accretion models for T Tauri stars. 1: Balmer line profiles without rotation. *Astrophys. J.* 426:669-687.
- Hartmann, L. 1995. Observational Constraints on Disk Winds. In

- Circumstellar Disks, Outflows and Star Formation. Rev. Mexicana Astron. Astrof. Serie de Conferencias.* 1:285-291.
- Hartmann, L. and Kenyon, S. J. 1996. The FU Orionis phenomenon. *Annu. Rev. Astron. Astrophys.* 34:207-240.
- Hartmann, L., Cassen, P. and Kenyon, S. J. 1997. Disk Accretion and the Stellar Birthline. *Astrophys. J.* 475:770-785.
- Hartmann, L., Calvet, N., Gullbring, E. and D'Alessio, P. 1988. Accretion and the Evolution of T Tauri Disks. *Astrophys. J.* 495:385-400.
- Herbig, G. H. 1977. Eruptive phenomena in early stellar evolution. *Astrophys. J.* 217:693-715.
- Hodapp, K-W, Hora, J. L., Rayner, J. T., Pickles, A. J., and Ladd, E. F., 1996. An outburst of a deeply embedded star in Serpens. *Astrophys. J.* 468:861-870.
- Jensen, E. L. N., Mathieu, R. D. and Fuller, G. A. 1994. A connection between submillimeter continuum flux and separation in young binaries. *Astrophys. J.* 429:L29-L32.
- Kawazoe, E. and Mineshige, S. 1993. Unstable accretion disks in FU Orionis stars. *Publ. Astron. Soc. Pacific* 45:715-725.
- Kenyon, S. J. and Hartmann, L. 1987. Spectral energy distributions of T Tauri stars - Disk flaring and limits on accretion. *Astrophys. J.* 323:714-733.
- Kenyon, S. J. and Hartmann, L. 1995. Pre-Main-Sequence Evolution in the Taurus-Auriga Molecular Cloud. *Astrophys. J. Suppl.* 101:117-171.
- Kenyon, S. J. and Hartmann, L. 1996. The FU Orionis Phenomenon. *Ann. Rev. Astron. Astrophys.* 34:207-240.
- Kenyon, S. J., Hartmann, L., Strom, K. M. and Strom, S. E. 1990. An IRAS survey of the Taurus-Auriga molecular cloud. *Astron. J.* 99:869-887.
- Kenyon, S.J., Calvet, N., and Hartmann, L. 1993a. The embedded young stars in the Taurus-Auriga molecular cloud. I. Models for the spectral energy distribution. *Astrophys. J.* 414:676-694.
- Kenyon, S.J., Whitney, B., A., Gomez, M., and Hartmann, L. 1993b. The embedded young stars in the Taurus-Auriga molecular cloud. II - Models for scattered light images. *Astrophys. J.* 414:773-792.
- Kenyon, S., Gomez, M., Marzke, R. O. and Hartmann, L. 1994. New pre-main-sequence stars in the Taurus-Auriga molecular cloud. *Astron. J.* 108:251-261.
- Kenyon, S., J., Yi, I., and Hartmann, L. 1996. A Magnetic Accretion Disk Model for the Infrared Excesses of T Tauri Stars. *Astrophys. J.* 462:439-455.
- Königl, A. 1989. Self-similar models of magnetized accretion disks. *Astrophys. J.* 342:208-223.
- Königl, A. 1991. Disk accretion onto magnetic T Tauri stars. *Astrophys. J. Lett.* 370:L39-L43.

- Larson, R. B. 1984. Gravitational torques and star formation. *Mon. Not. Roy. Astron. Soc.* 206:97-207.
- Lin, D. N. C. and Bodenheimer, P. 1982. On the evolution of convective accretion disk models of the primordial solar nebula. *Astrophys. J.* 262:768-779.
- Lin, D. N. C. and Papaloizou, J. C. B. 1985. On the dynamical origin of the solar system. In *Protostars & Planets II*, eds. D. C. Black and M. S. Matthews (Tucson: Univ. of Arizona Press), pp. 981-107.
- Lynden-Bell, D. and Pringle, J. E. 1974 The evolution of viscous discs and the origin of the nebular variables. *Mon. Not. Roy. Astron. Soc.* 168:603-638.
- Mathieu, R., Adams, F. C., Fuller, G. A., Jensen, E. L., N., Koerner, D. W. and Sargent, A. Submillimeter Continuum Observations of the T Tauri Spectroscopic Binary GW Orionis. *Astron. J.* 109:2655-2669.
- McCaughrean, M. J. and O'Dell, C. R. 1996 Direct Imaging of Circumstellar Disks in the Orion Nebula. *Astron. J.* 111:1977-1986.
- McCaughrean, M. J., Chen, H., Bally, J., Erickson, Ed, Thompson, R., Rieke, M., Schneider, G., Stolovy, S. and Young, E. 1998. High-resolution near-infrared imaging of the Orion 114-426 silhouette disk. *Astrophys. J. Lett.* 492:L157-161.
- Meyer, M. R., Calvet, N. and Hillenbrand, L. A. 1997. Intrinsic Near-Infrared Excesses of T Tauri Stars: Understanding the Classical T Tauri Star Locus. *Astrophys. J.* 114:288-300.
- Muzerolle, J., Calvet, N. and Hartmann, L. 1998a. Magnetospheric Accretion Models for the Hydrogen Emission Lines of T Tauri Stars. *Astrophys. J.* 492:743-753.
- Muzerolle, J., Hartmann, N. and Calvet, N. 1998b. Emission-Line Diagnostics of T Tauri Magnetospheric Accretion. I. Line Profile Observations. *Astron. J.* 116:455-468.
- Muzerolle, J., Hartmann, N. and Calvet, N. 1998c. A Br $\gamma$  Probe of Disk Accretion in T Tauri Stars and Embedded Young Stellar Objects. *Astrophys. J.* (in press).
- Moriarty-Schieven, G.H. and Snell, R. 1988. High-resolution images of the L1551 molecular outflow. II. Structure and kinematics. *Astrophys. J.* 332:364-378.
- Osterloh, M. and Beckwith, S. V. W. 1995. Millimeter-wave continuum measurements of young stars. *Astrophys. J.* 439:288-302.
- Pringle, J. E. 1981. Accretion discs in astrophysics. *Ann. Rev. Astron. Astrophys.* 19:137-162.
- Pringle, J. E. 1991. The properties of external accretion discs. *Mon. Not. Roy. Astron. Soc.* 248: 754-759.
- Pudritz, R. E. and Norman, C. A. 1983. Centrifugally driven winds from contracting molecular disks. *Astrophys. J.* 274:677-697.
- Reipurth, B. 1985. Herbig-Haro objects and FU Orionis eruptions -

- The case of HH 57. *Astron. Astrophys.* 143:435-442.
- Reipurth, B. and Aspin, C. 1997. Infrared spectroscopy of Herbig-Haro energy sources. *Astron. J.* 114:2700-2707.
- Rucinski, S. M. 1985, Iras observations of T Tauri and post-T Tauri stars. *Astron. J.* 90:2321-2330.
- Rydgren, A. E. and Zak, D. S. 1987. On the spectral form of the infrared excess component in T Tauri systems. *Publ. Astron. Soc. Pacific* 99:141-145.
- Sandell, G. and Aspin, C. 1998. PP13S, a young, low-mass FU Orionis-type pre-main sequence star. *Astron. Astrophys.* 333:1016-1025.
- Shakura, N. I. and Sunyaev, R. A. 1973. Black holes in binary systems. Observational appearance. *Astron. Astrophys.* 24:337-355.
- Shu, F. H., Adams, F. C. and Lizano, S. 1987. Star formation in molecular clouds - Observation and theory. *Ann. Rev. Astron. Astrophys.* 25:23-81.
- Shu, F. H., Najita, J., Ostriker, E., Wilkin, F., Ruden, S. P. and Lizano, S. 1994. Magnetocentrifugally driven flows from young stars and disks. 1: A generalized model. *Astrophys. J.* 429:781-796.
- Simon, M., Ghez, A. M., Leinert, C. H., Cassar, L., Chen, W. P., Howell, R. R., Jameson, R. F., Matthews, K., Neugebauer, G. and Richichi, A. 1995. A lunar occultation and direct imaging survey of multiplicity in the Ophiuchus and Taurus star-forming regions. *Astrophys. J.* 443:625-637.
- Stahler, S. W. 1988. Deuterium and the stellar birthline. *Astrophys. J.* 332:804-825.
- Staude, H. J. and Neckel, T. 1991. RNO 1B - A new FUor in Casiopeia. *Astron. Astrophys.* 244: L13-L16.
- Stepinski, T. F. 1998. Diagnosing Properties of Protoplanetary Disks from their evolution. *Astrophys. J.* in press.
- Stone, J.M., Hawley, J.F., Gammie, C. F., and Balbus, S.A. 1996. *Astrophys. J.* 463:656.
- Valenti, J. A., Basri, G. and Johns, C. M. 1993 Tauri stars in blue. *Astron. J.* 106:2024-2050.

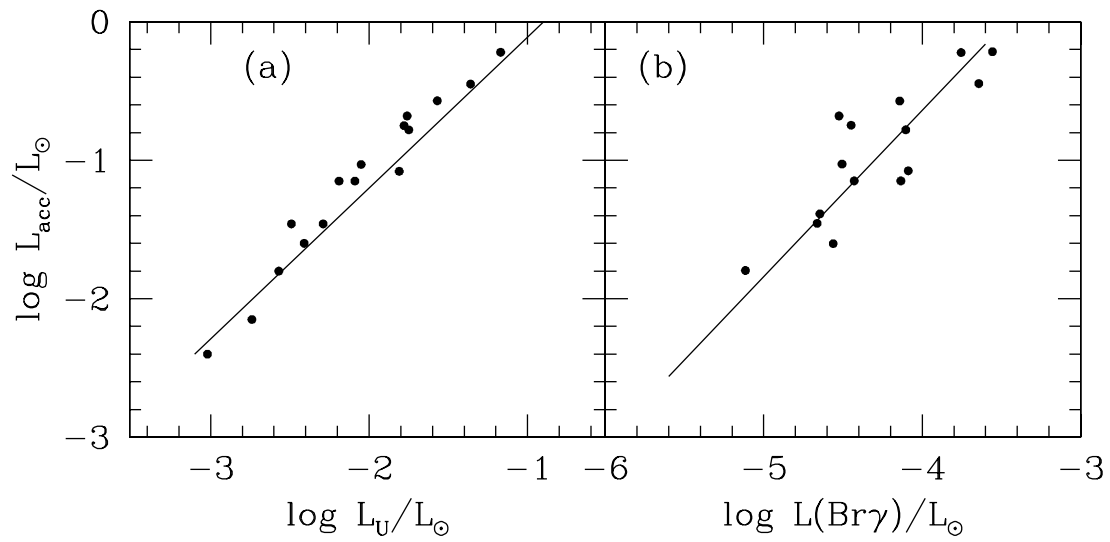


Figure 1. Relationship between accretion luminosity and (a) the excess luminosity in the U band, and (b) the luminosity in  $\text{Br}\gamma$  for a sample of CTTS in Taurus. Data from Gullbring et al. (1997) and Muzerolle et al. (1998c).

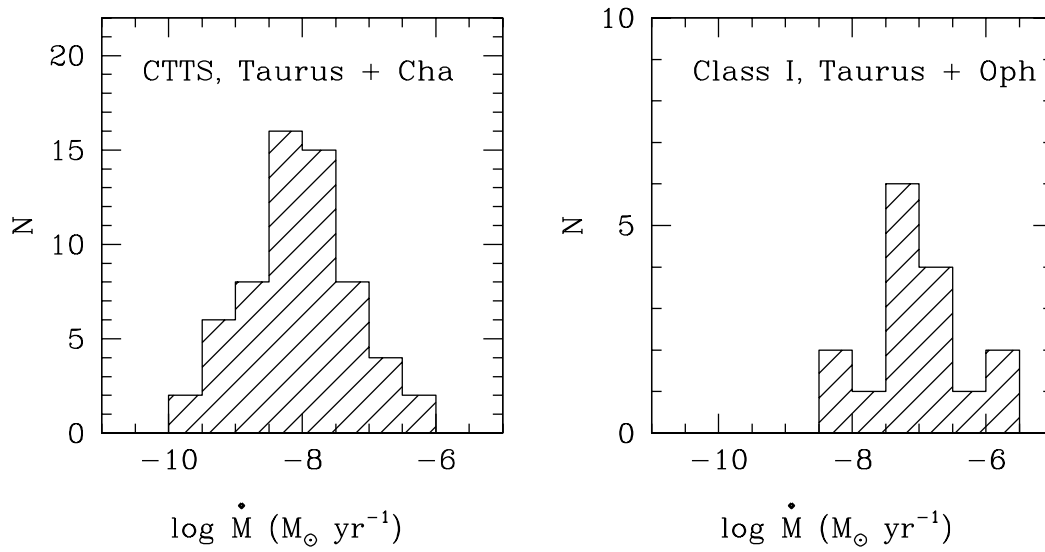


Figure 2. Histogram showing the distribution of mass accretion rates. (a) For T Tauri stars in Taurus and Cha I, with  $\dot{M}$  determined from blue spectra or U magnitudes, and (b) For Class I sources in Taurus and  $\rho$  Oph, determined from  $\text{Br}\gamma$  measurements.

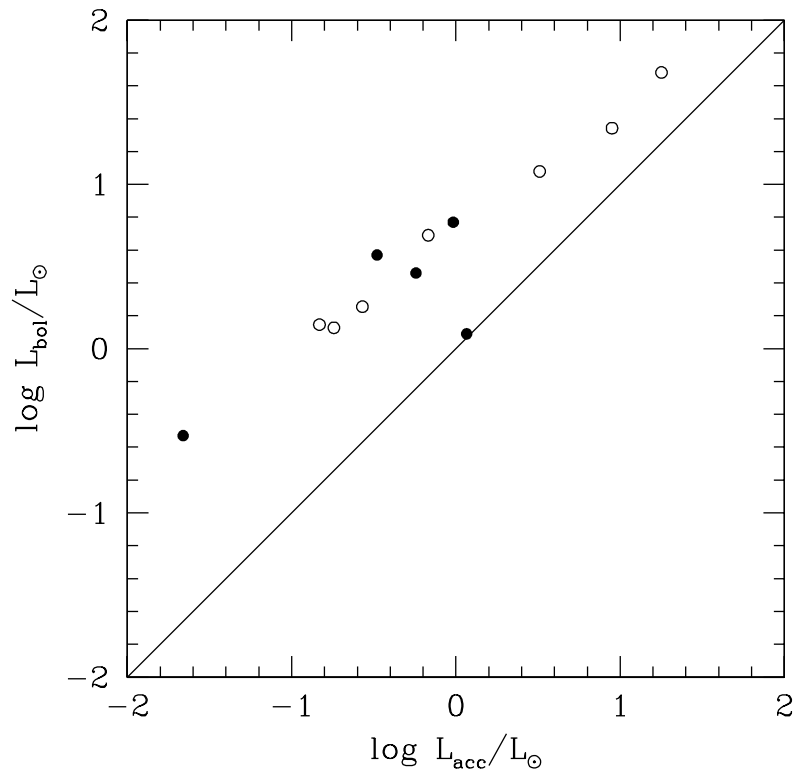


Figure 3. Relationship between accretion luminosity and bolometric luminosity for Class I sources in Taurus (filled circles) and in  $\rho$  Oph (open circles) (from Muzerolle et al. 1998c).



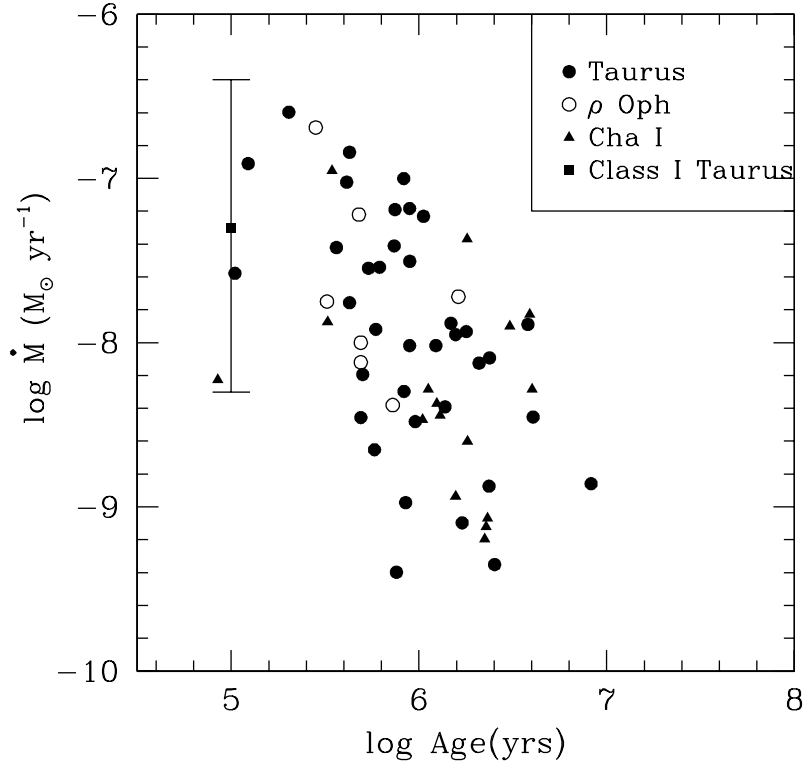


Figure 4. Observed mass accretion rate vs. age for CTTS in Taurus, Cha I, and  $\rho$  Oph. Mass accretion rates have been obtained by the methods described in section II. Ages for the CTTS have been estimated from the position in the HR diagram and comparison with the theoretical tracks from D'Antona and Mazitelli (1994, CMA case). Luminosities and spectral types were taken from Kenyon and Hartmann (1995) for Taurus, Gauvin and Strom (1992) for Cha I, and Greene and Meyer (1995) for  $\rho$  Oph. The mean and dispersion of the estimated mass accretion rates for Class I sources is also shown for comparison (see II.C). The mean age for the Class I sources is assumed to be 0.1 Myr.

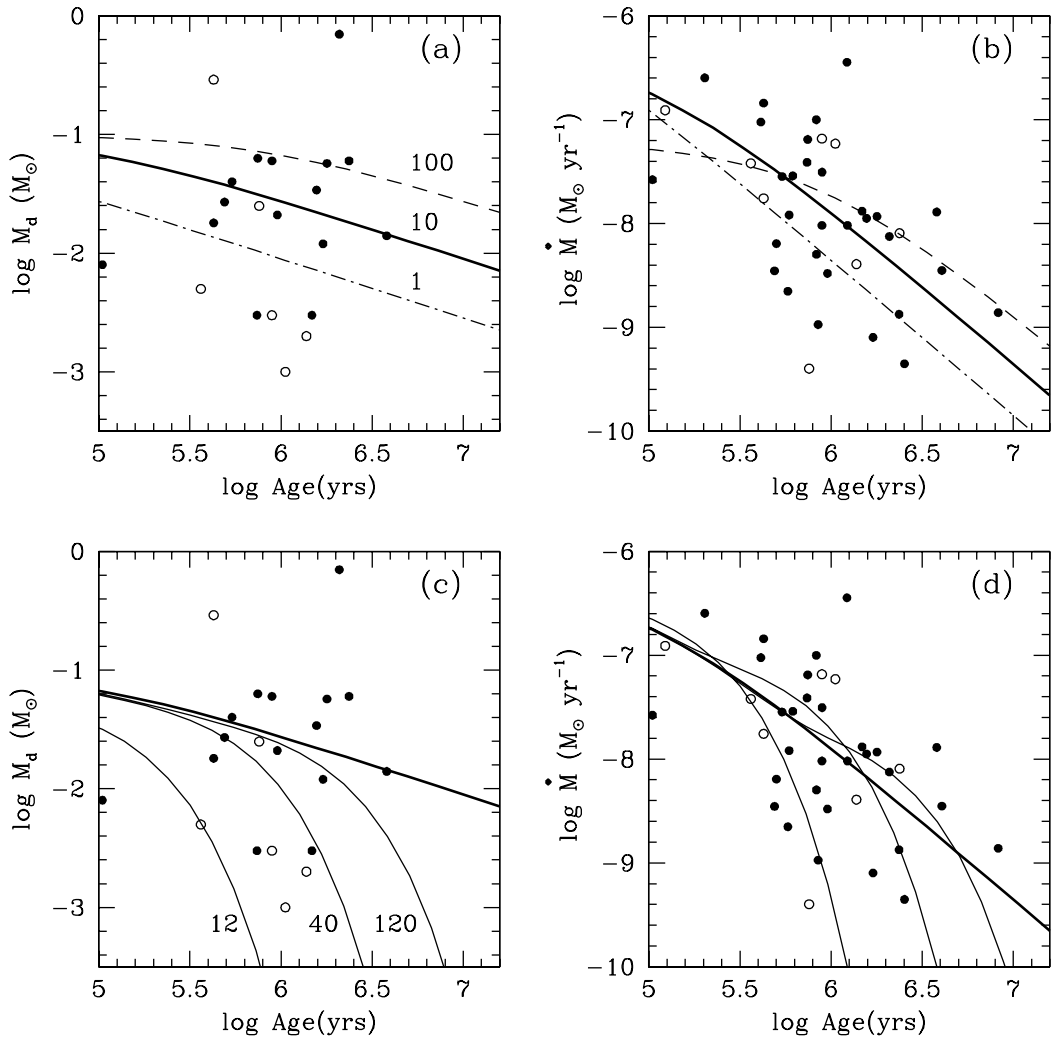


Figure 5. Similarity solution for disk evolution, with  $\nu \propto R$ , compared to observations. Upper panels: Evolution for isolated disks. (a) Disk mass vs. time. (b)  $\dot{M}$  vs. time. Models shown have initial disk mass of  $0.1 M_\odot$  and initial disk radii (marked): 1, 10, and 100 AU. Lower panels: Evolution with binary companions. (c) Disk mass vs. time. (d)  $\dot{M}$  vs. time. Models are shown for initial disk mass and radius of  $0.1 M_\odot$  and 10 AU, and for three binary separations: 30 AU, 100 AU, and 300 AU (corresponding to truncation radii of 12, 40, and 120 AU, marked). The corresponding evolution for the isolated disk is shown for comparison (heavy line). Binaries indicated by open circles.

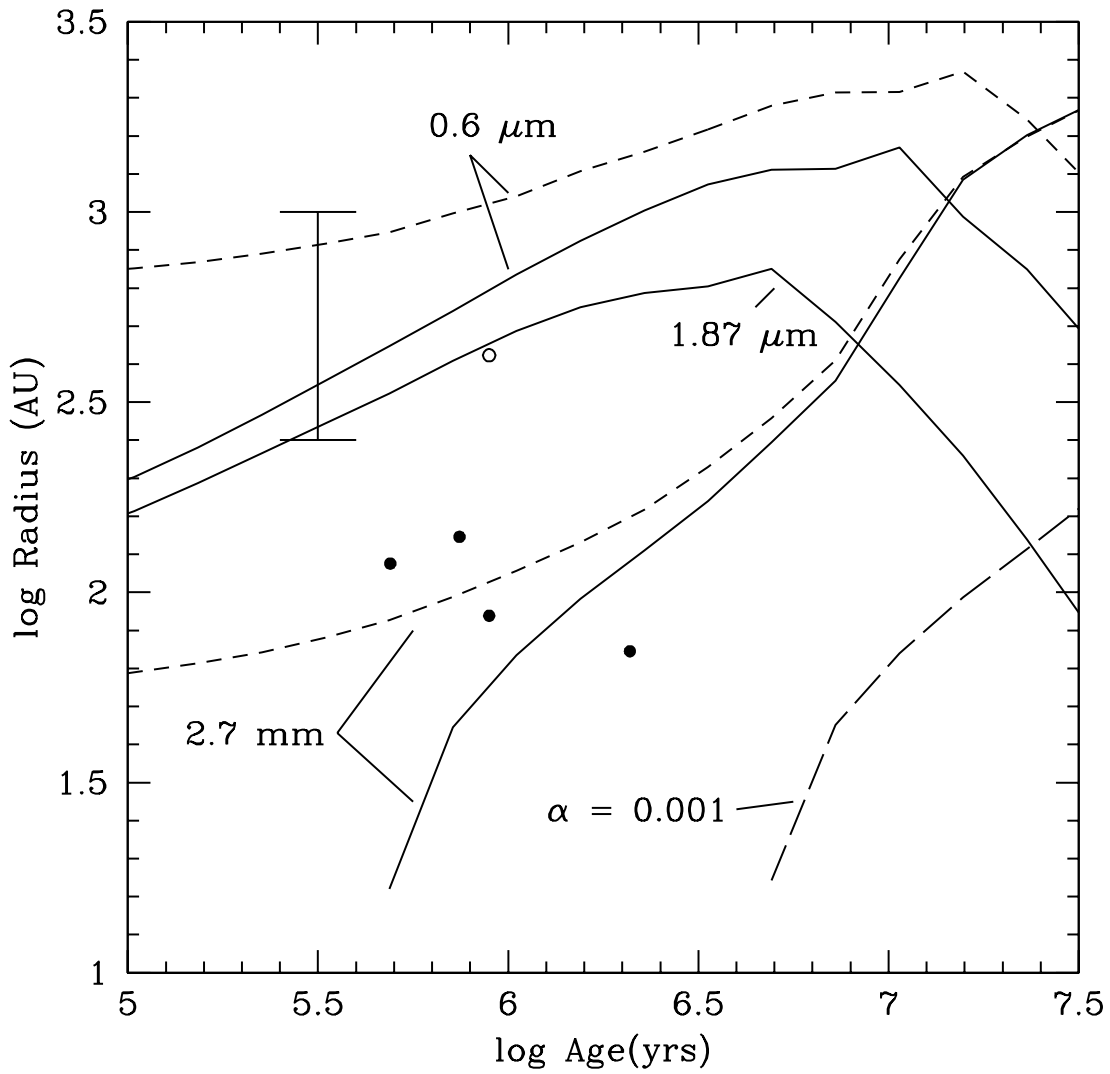


Figure 6. Characteristic disk sizes for viscous evolution as observed at  $0.6 \mu\text{m}$ ,  $1.87 \mu\text{m}$ , and  $2.7 \text{ mm}$ . Models are shown for an initial mass of  $0.1 M_{\odot}$  and initial radii 10 AU (solid) and 100 AU (short dashes). A model with initial radii 10 AU but  $\alpha = 0.001$  is shown for comparison (long dashes). Data from Dutrey et al. (1996) are shown as circles, and the error bar indicates the range of sizes measured in the disks seen in silhouettes in the Orion Nebula cluster (McCaughrean and O'Dell 1996). Binaries are indicated by open circles. See text.

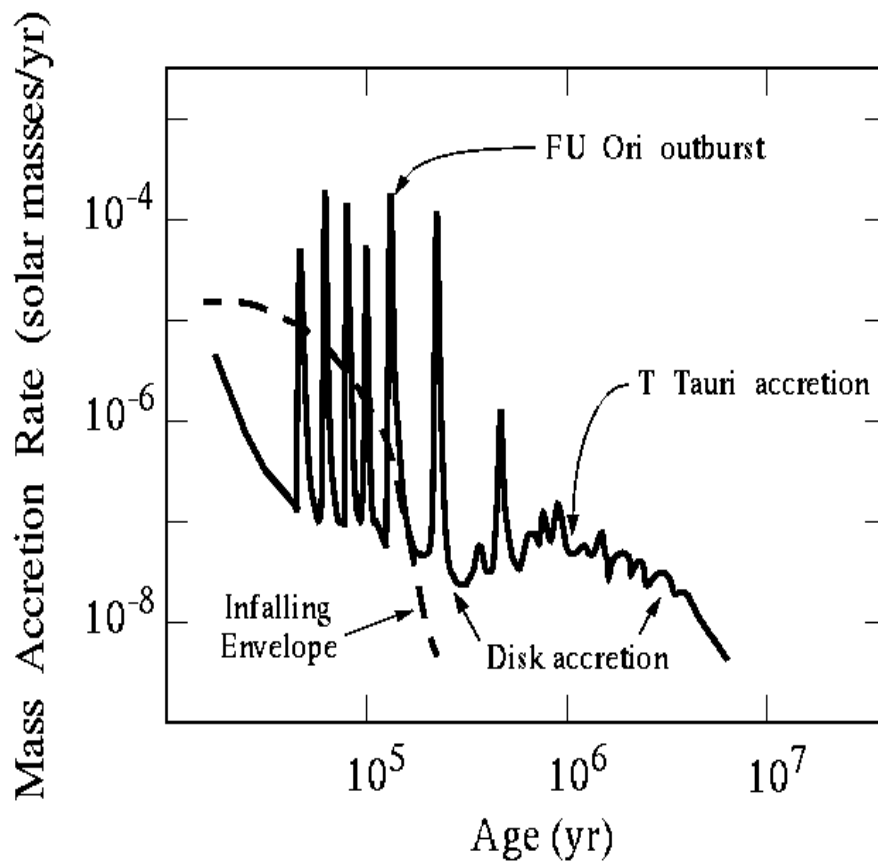


Figure 7. Sketch of disk evolution with time, summarizing the ideas presented in this chapter. The disk remains most of the time in a quiescent state, punctuated by episodes of high  $\dot{M}$  as long as the envelope feeds mass to the disk. When infall ceases, the disk evolves viscously and  $\dot{M}$  slowly decreases with time.